

Measurements on Iris-Structures with Rectangular Holes *

M. Kurz, P. Hülsmann, H. Klein, A. Schempp

Institut für Angewandte Physik

Robert-Mayer-Straße 2-4, D - 6000 Frankfurt am Main, Fed. Rep. of Germany

Abstract

By replacing the irises in an electron linac by rectangular slots one gets a structure capable of focussing/defocussing an electron beam. Therefore this kind of iris-geometry could be employed alone or in combination with conventional magnetic quadrupoles for transversal focussing in future linear-colliders.

A three-cell structure with rectangular "irises" was designed and tuned to $v_{ph}=c$ at TM_{010} $2\pi/3$ -mode. Perturbation measurements were performed in order to determine the fields and focussing strength of the structure.

I. INTRODUCTION

All schemes proposed for future e^+e^- -linear-colliders are featuring travelling-wave structures of iris-type for the main linac. Operating frequencies are proposed to be in the range between 11.47GHz (SLC) and 29GHz (CLIC). In this frequency regime wake field effects cannot be neglected; longitudinal wakes scaling with ω^2 , transversal wakes scaling with ω^3 [1]. The final-focus luminosity needed for experiments is about $10^{33} \text{ cm}^{-2} \text{ s}^{-1}$. This means that beam quality has to be maintained over rather long distances (e.g. 12.5km for the CLIC main-linac) and additional transversal focussing will be required. One way to achieve the focussing is to apply external magnetic quadrupoles. The rectangular "irises" investigated in this paper could possibly be an alternative or supplement to conventional methods, combining a high accelerating gradient with the potential of considerable transverse focussing power [2,3]. The principle is the same as in the RFQ-scheme frequently used for accelerating low-energy ions.

II. THEORETICAL ASPECTS OF RF-FOCUSSING

We assume a TM_{01} -wave travelling at $v=c$ through a loaded waveguide operating in $\pi/2$ -mode for the sake of easier understanding

(see Figure 1). The results are valid for any other operating mode too.

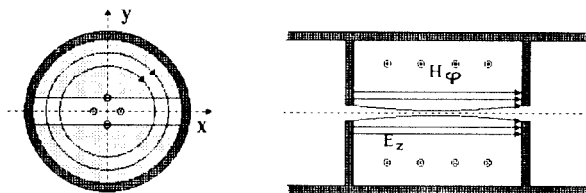


Figure 1 RF-quadrupole in $\pi/2$ -mode

The iris is replaced by a narrow slit of the size of the cavity diameter oriented in X-direction. Its height is chosen such that the magnetic field behind the screen remains undisturbed. The E_z field is assumed to be of the form

$$E_z = E_0 \cos(\omega t - kz). \quad (1)$$

Because of the geometry of the slot $\partial H_\phi / \partial \phi = 0$. From Maxwell's equation using cylindrical coordinates we find

$$H_\phi = -\frac{\epsilon r \omega}{2} E_0 \sin(\omega t - kz). \quad (2)$$

The boundary conditions allow no X-component of the electrical field inside the screen. From $\text{div} E = 0$ we get the Y-component of the electric field

$$E_y = -y k E_0 \sin(\omega t - kz). \quad (3)$$

A particle travelling at $v \approx c$ and entering the structure at a certain phase Φ with respect to the RF will maintain this phase on its way through the structure. In the X-direction the particle will only experience magnetic forces; there will be additional electrical forces in the Y-direction. Finally we find

$$F_x = \frac{q \omega}{2 c} x E_0 \sin(\Phi), \quad (4)$$

$$F_y = -\frac{q \omega}{2 c} y E_0 \sin(\Phi),$$

and the focussing gradients

$$G_x = \frac{\omega}{2 c^2} E_0 \sin(\Phi), \quad (5)$$

$$G_y = -G_x.$$

* work supported by BMFT under contract No. 055FM111

An accelerating section of length l then forms a microwave-quadrupole of focal length f given by

$$f^{-1} = \frac{cG l}{U}, \quad (6)$$

eU being the particle energy.

This derivation shows that under such idealized conditions this structure forms a rf-quadrupole.

III. EXPERIMENTS

A. Experimental setup

A three-cell structure was designed and tuned to $v_{ph} \approx c$ in the TM_{010} $2\pi/3$ -mode. A sketch of the geometry used is given in Figure 2.

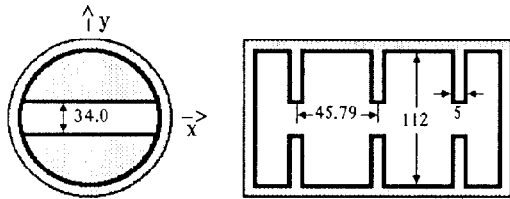


Figure 2 Structure geometry (dimensions in mm)

For the measurements a computer-controlled test stand was used, allowing for data acquisition and further processing (see Figure 3). For the reason of eliminating oscillations of the bead the cavity was moved. The catch of the bead was made adjustable on either side of the test bench in order to allow for aligning the bead with the cavity-axis.

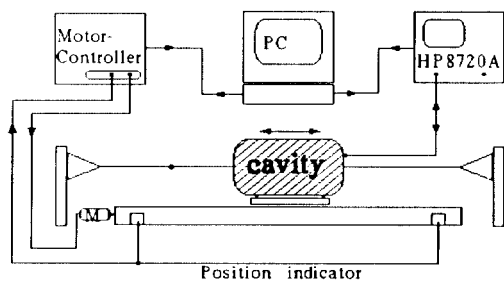


Figure 3 Experimental setup

For measuring the electric field a thin dielectric needle (Al_2O_3) was used. The bead was first calibrated in TM_{010} pillbox cavity of well known geometry.

B. Experimental results

The cavity was tuned to $v_{ph} \approx c$ by gradually

adjusting the height of the slot. The optimum was found for a 34 mm aperture.

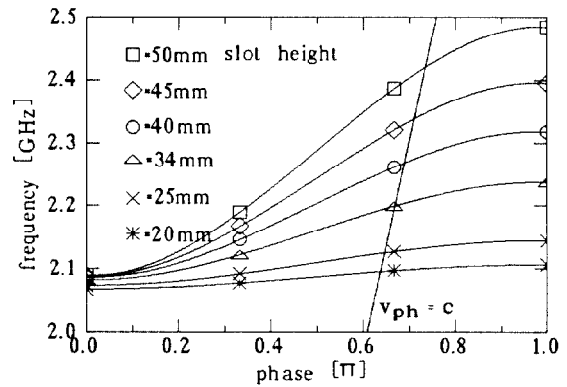


Figure 4 Brillouin-diagram of the structure for several apertures

As can be seen from the Brillouin-diagram in Figure 4 the coupling in the structure is still predominantly electric. Group velocity v_g/c is about 6.5% in the operating mode.

The E_z -field was measured on axis and for several off-axis positions in the X-Z-plane and the Y-Z-plane. The electric field is plotted versus the Z-position of the bead (see Figures 5 and 6).

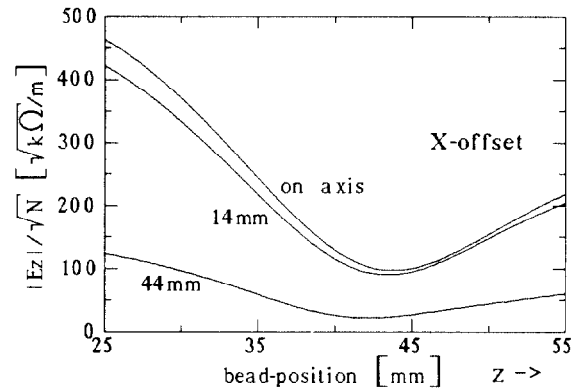


Figure 5 E-field versus bead position. Parameter: Bead offset in X-direction. The middle of screen is at $z=42$ mm

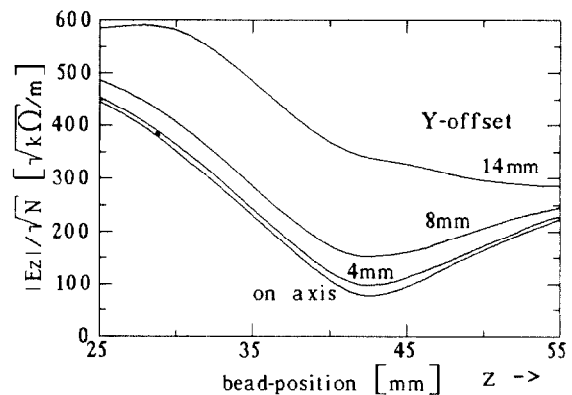


Figure 5 E-field versus bead position. Parameter: Bead offset in X-direction. The middle of screen is at $z=42$ mm

According to the analytical approach the focussing in the X-plane is due to the magnetic field. Instead of measuring the H_φ -component we can apply to the $E_z(x)$ field which is proportional to $-H_\varphi$. In the Y-plane the relevant $E_z(z)$ field was recorded as well.

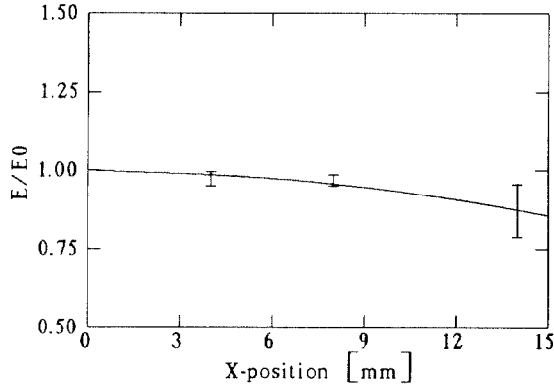


Figure 7 Normalized E_z -field vs. X-offset

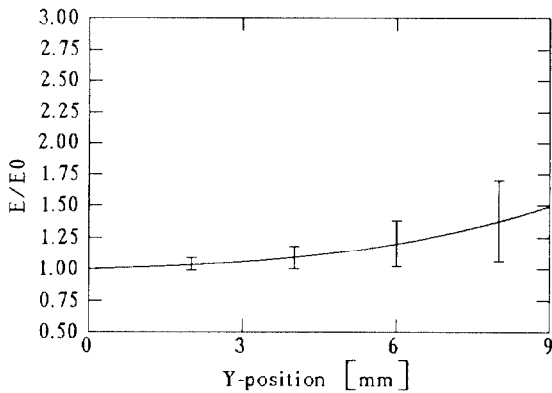


Figure 8 Normalized E_z -field vs. Y-offset

It can be seen, that the ratio E/E_0 is close to unity only for small offsets. While the change is modest for the X-offset due to the decay of the field towards the cavity wall it shows that in the Y-direction the effect of the edges causes a steeper curve.

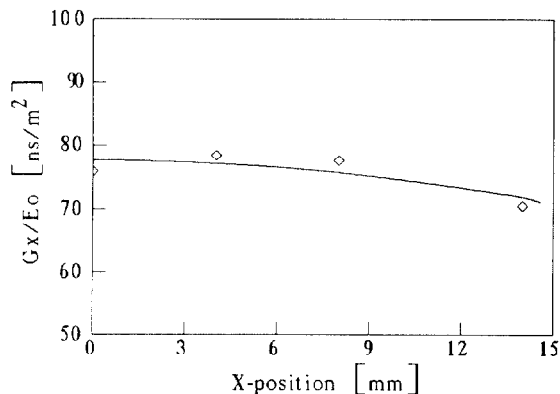


Figure 9 Normalized focussing gradient G_x/E_0

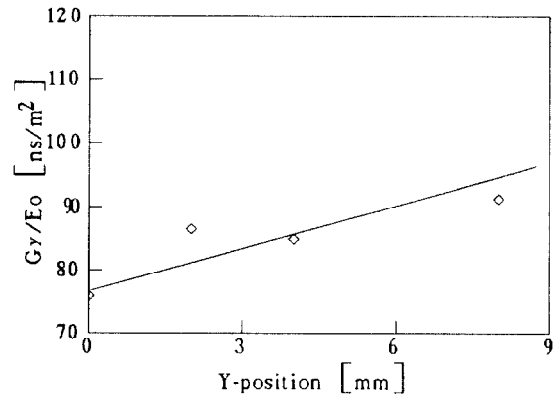


Figure 10 Normalized focussing gradient G_y/E_0

The normalized focussing gradients for the X- and Y-direction are given in Figure 9 and 10.

IV. CONCLUSIONS

The transverse focussing gradients of the examined structure match the analytical estimate [2] of 76.9 ns/m^2 nearly exactly. Also the results correspond well to the ones obtained by MAFIA-calculations done by I. Wilson and H. Henke [4]. Scaled to 29GHz we find a normalized gradient of about $0.98 \mu\text{s/m}^2$ which would be equivalent to 27 T/m at 20° rf-phase and 80 MV/m effective accelerating field.

V. REFERENCES

- [1] H. Henke, CLIC Note 100, Geneva, 1989
- [2] W. Schnell, CERN-LEP-RF/87-24, CLIC Note 34, Geneva, March 1987
- [3] R. B. Palmer, Private Communication
- [4] I. Wilson, H. Henke, CLIC Note 62, Geneva, May 1988